Journal of Alloys and Compounds 509 (2011) 7915–7921

Contents lists available at ScienceDirect

Journal of Alloys and Compounds

journal homepage: www.elsevier.com/locate/jallcom

Structural characterization of layered $LiNi_{0.85-x}Mn_xCo_{0.15}O_2$ with $x = 0$, 0.1, 0.2 and 0.4 oxide electrodes for Li batteries

Yi-Jie Gu [a,b,*], Yun-Bo Chen [c], Hong-Quan Liu [a], Yan-Ming Wang [a], Cui-Ling Wang [a,d], Hui-Kang Wu [a]

[a] College of Materials Science and Engineering, Shandong University of Science and Technology, Qingdao 266510, China
[b] Department of Chemistry, University of California, Riverside, CA 92521, USA
[c] Advanced Manufacture Technology Center, China Academy of Machinery Science and Technology, Beijing 100044, China
[d] Department of Materials Engineering, Jining Technology College, Jining, Shandong 272013, China

ARTICLE INFO

Article history:
Received 20 January 2011
Received in revised form 8 May 2011
Accepted 9 May 2011
Available online 14 May 2011

Keywords:
The ordering of Mn^{4+} with Ni^{2+} and Mn^{4+} with Li^+
Mn-doping
L_{M-O}
Structural characterization
Li batteries

ABSTRACT

We report the synthesis of $LiNi_{0.85-x}Co_{0.15}Mn_xO_2$ positive electrode materials from $Ni_{0.85-x}Co_{0.15}Mn_x(OH)_2$ and Li_2CO_3. XRD and XPS are used to study the effect of Mn-doping on the microstructures and oxidation states of the $LiNi_{0.85-x}Co_{0.15}Mn_xO_2$ materials. The analysis shows that Mn-doping promotes the formation of a single phase. With increasing substitution of Mn ions for Ni ions, the lattice parameter a decreases, while the lattice parameters c and c/a increase. XPS revealed that the oxidation states of Ni, Co and Mn in $LiNi_{0.85-x}Co_{0.15}Mn_xO_2$ compounds (where $x = 0.1$, 0.2 and 0.4) were +2/+3, +3 and +4. The substitution of Mn ions for Ni ions induces a decrease in the average oxidation state of Ni. Because the substitution of Mn for Ni ions is complex, the extent of the changes between the lattice parameter and L_{M-O} differ. The occupation of Ni in Li sites is affected by the ordering of Mn^{4+} with Ni^{2+} and Mn^{4+} with Li^+.

1. Introduction

Stoichiometric $LiNiO_2$ is difficult to synthesize [1]. During cycling, lithium occupies nickel sites to cause structural instability and capacity deterioration [2]. Cobalt and manganese ions have been considered as possible candidates for partial substitution of nickel to help overcome the unsatisfactory characteristics of $LiNiO_2$ [3–5]. Cobalt ions suppressed the Jahn–Teller distortion in the deintercalation process of lithium. This resulted in significant stabilization of the structure and good cycling performance of $LiNi_{1-x}Co_xO_2$ [6]. However, heavy doping with cobalt increases the fabrication cost and toxicity of lithium nickel oxide. There are also reports of manganese-doped lithium nickel oxide, $LiNi_{1-x}Mn_xO_2$, which shows safety characteristics even when being charged at 4.6 V. Materials containing $LiNiO_2$ doped with a single ion do not exhibit satisfactory improvement in performance over lithium nickel oxide. Thus, researchers began to study lithium nickel oxide doped with multiple ions. The new layered structure compounds $LiNi_{1-x-y}Co_yMn_xO_2$ and $LiNi_xCo_{1-2x}Mn_xO_2$ were developed and these demonstrate better overall performance [7–9].

In this study, $LiNi_{0.85}Co_{0.15}O_2$ was doped with manganese ions to improve its cost effectiveness and performance characteristics. The series of Mn-doped $LiNi_{0.85-x}Co_{0.15}Mn_xO_2$ ($x = 0$, 0.1, 0.2 and 0.4) powders were synthesized by coprecipitation. We studied how doping with different proportions of manganese ions changed the structure and oxidation states of the $LiNi_{0.85-x}Co_{0.15}Mn_xO_2$ compounds using X-ray diffraction (XRD) and X-ray photoelectron spectroscopy (XPS).

2. Experimental

The metal hydroxide $Ni_{0.85-x}Co_{0.15}Mn_x(OH)_2$ ($x = 0$, 0.1, 0.2 and 0.4) precursors were prepared by coprecipitation. $Ni(NO_3)_2{\cdot}6H_2O$, $Co(NO_3)_2{\cdot}6H_2O$, $Mn(NO_3)_2$ (mass concentration, 50%), NaOH and NH_4OH were used as the starting materials. Mixtures of $Ni(NO_3)_2{\cdot}6H_2O$, $Co(NO_3)_2{\cdot}6H_2O$, $Mn(NO_3)_2$ (cationic ratio of Ni:Co:Mn = 0.85−x:0.15:x) were dissolved in distilled water to form aqueous solutions with a concentration of 1.0 mol dm^{-3}. This solution was slowly added dropwise into a stirred solution of NH_4OH and NaOH (aqueous, pH = 10.5). At the same time, further NH_4OH and NaOH solution was added at a constant rate to maintain a pH of 10.5. The temperature was kept at 50 °C to accelerate the rate of coprecipitation. After the reactants had been added, the solution was stirred for a further 20 h. The resulting precipitate was filtered and washed three times with distilled water to ensure that any residual ions (such as Na^+ or NO_3^-) were completely removed. The precipitate was then dried in air at 80 °C for 12 h, giving the $Ni_{0.85-x}Co_{0.15}Mn_x(OH)_2$ precursor. The solids were pre-calcined with Li_2CO_3 at 650 °C in air for 5 h to impregnate Li_2CO_3 into the matrix, and then calcined at 900 °C for 10 h in air. XRD measurements of the $LiNi_{0.85-x}Co_{0.15}Mn_xO_2$ materials were carried out using an X-ray diffractometer (Bruker, D8 ADVANCE, Germany) equipped with a diffracted beam monochromator. XRD data were collected in the range of 10–70° (2θ) using a

* Corresponding author at: College of Materials Science and Engineering, Shandong University of Science and Technology, Qianwangang Road 579#, Qingdao 266510, China. Tel.: +86 532 88032993; fax: +86 532 86057098.
E-mail address: guyijie@sdust.edu.cn (Y.-J. Gu).

0925-8388/$ – see front matter © 2011 Elsevier B.V. All rights reserved.
doi:10.1016/j.jallcom.2011.05.024

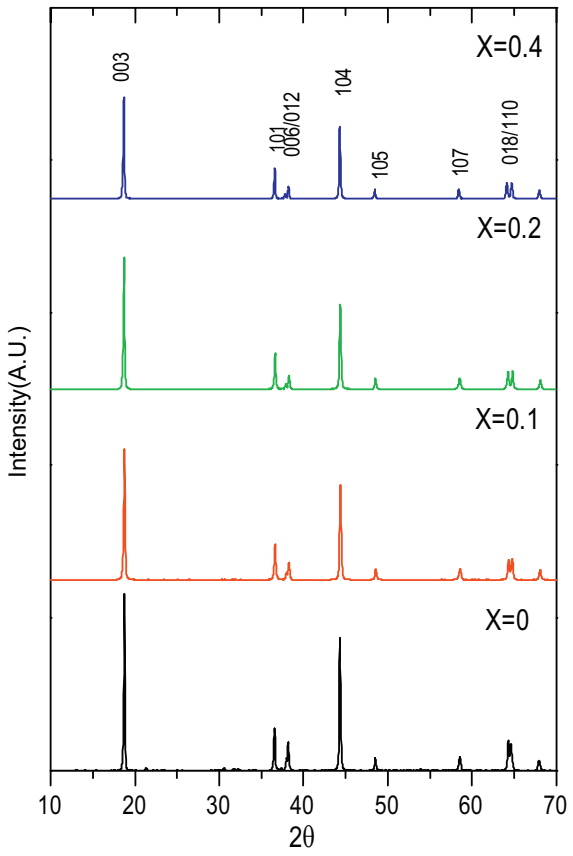

Fig. 1. XRD patterns of the $LiNi_{0.85-x}Co_{0.15}Mn_xO_2$ compounds ($x = 0$, 0.1, 0.2 and 0.4).

step-scan method with a step size of 0.02° and a counting time of 1 s per step. The structural refinements were performed using FullProf. The chemical compositions of the synthesized materials were determined by an inductively coupled plasma spectrometer (ICP: Agilent7500a, Japan). XPS data for the materials were obtained on a Thermo ESCALAB 250 (USA) spectrometer using a monochromatic Mg X-ray source.

3. Results

Fig. 1 shows the X-ray diffraction patterns of the positive electrode materials $LiNi_{0.85-x}Co_{0.15}Mn_xO_2$ ($x = 0$, 0.1, 0.2 and 0.4). The Miller indices of the samples are based on the hexagonal α-$NaFeO_2$ structure (space group: *R*-3*m*, no. 166). As the content of Mn ions was increased, the positions of the main diffraction peaks showed little variation, but their intensities changed. The intensities of the (0 0 3) and (1 0 4) crystal face diffraction peaks of $LiNi_{0.85}Co_{0.15}O_2$ are higher than those of any manganese-doped compounds. The (0 0 6)/(0 1 2) and (0 1 8)/(1 1 0) doublets are increasingly separated as the Mn content increases. The small peaks between diffraction angles 20–40° in the $LiNi_{0.85}Co_{0.15}O_2$ diffraction curve indicate the presence of a small amount of an impurity. The small diffraction lines between 20° and 30° could be attributed to Li_2CO_3. There is a small diffraction line at 37° which may be caused by a Co_2NiO_4 impurity. It can be seen from the XRD patterns that none of the manganese-doped materials contain impurities. The single phase structure forms more readily for the Mn-doped materials $LiNi_{0.85-x}Co_{0.15}Mn_xO_2$ ($x = 0.1$, 0.2 and 0.4) than for the undoped material $LiNi_{0.85}Co_{0.15}O_2$ by the preparation method in air.

The X-ray diffraction patterns of the $LiNi_{0.85-x}Co_{0.15}Mn_xO_2$ ($x = 0$, 0.1, 0.2 and 0.4) compounds were refined. The X-ray diffraction pattern of $LiNi_{0.65}Co_{0.15}Mn_{0.2}O_2$, together with its refinement, is shown in Fig. 2. Table 1 gives the structural parameters determined for the $LiNi_{0.85-x}Co_{0.15}Mn_xO_2$ materials ($x = 0$, 0.1, 0.2 and 0.4) from the refinement of their XRD data.

The actual ionic distribution of $LiNiO_2$ is represented as $[Li_{1-\delta-\omega}Ni_{\delta+\omega}{}^{2+}]_{3b}[Ni_{1-\delta}{}^{2+}Ni_{\delta-\omega}{}^{3+}Li_{\omega}]_{3a}O_2$ [10], due to the presence of the Ni ions in the Li layer. Refinement of the XRD pattern of $LiNi_{0.85}Co_{0.15}O_2$ led to a cationic distribution for the pristine material $(Li_{0.850}Ni_{0.150})_{3b}(Ni_{0.818}Li_{0.032}Co_{0.150})_{3a}O_2$. The high nickel content favors the loss of lithium from the oxide. Moreover, it is very difficult to oxidize Ni^{2+} to Ni^{3+} in air. This means that when $LiNi_{0.85}Co_{0.15}O_2$ is synthesized in air it tends to contain nickel ions in its lithium sites resulting in a lithium deficient, non-stoichiometric compound [7]. The XRD data for $LiNi_{0.85}Co_{0.15}O_2$ indicates that its formation under atmospheric conditions can lead to impurity and Ni^{2+} ions in Li ion sites. Previous research has shown that $LiNi_{0.9}Co_{0.1}O_2$ formed in oxygen can form a single phase with a low proportion of Ni^{2+} ions in Li ion sites [11]. When the fraction of manganese ions was 0.1, the formula $LiNi_{0.75}Mn_{0.1}Co_{0.15}O_2$ was shown to describe well the structure of $(Li_{0.926}Ni_{0.074})_{3b}(Ni_{0.676}Mn_{0.100}Li_{0.074}Co_{0.150})_{3a}O_2$ obtained from the refinement of the XRD data. Neutron powder diffraction (PDF) analysis of $Li[Ni_{1/3}Mn_{1/3}Co_{1/3}]O_2$ showed a nonrandom distribution of Ni and Mn cations in the TM layers, with Ni closer to Mn in the first coordination shell, and a random distribution of Co [12]. When the Mn content is increased to 0.2, the occupation of Ni^{2+} ions in the lithium layer is 0.057. This increases to 0.065 when the Mn content is increased to 0.4, so the formula $LiNi_{0.45}Mn_{0.4}Co_{0.15}O_2$ may be represented as $(Li_{0.935}Ni_{0.065})_{3b}(Ni_{0.385}Mn_{0.400}Li_{0.065}Co_{0.15})_{3a}O_2$

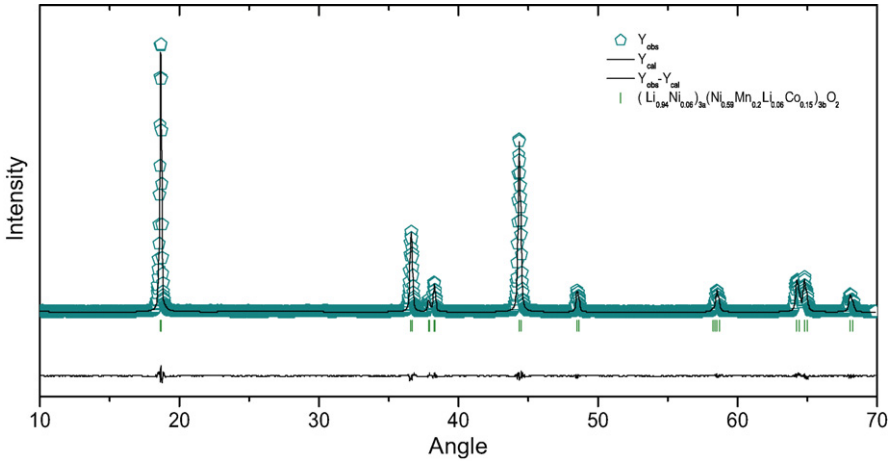

Fig. 2. Comparison of experimental and calculated XRD patterns of $LiNi_{0.65}Co_{0.15}Mn_{0.2}O_2$. Constraints: $n(Li)_{3a} + n(Ni)_{3a} = 1$; $n(Li)_{3b} + n(Ni)_{3b} + n(Mn)_{3b} = 1$.

Table 1
Structural parameters of $LiNi_{0.85-x}Co_{0.15}Mn_xO_2$ compounds (x = 0, 0.1, 0.2 and 0.4).

	$LiNi_{0.85}Co_{0.15}O_2$					$LiNi_{0.75}Mn_{0.1}Co_{0.15}O_2$	$LiNi_{0.65}Mn_{0.2}Co_{0.15}O_2$	$LiNi_{0.45}Mn_{0.4}Co_{0.15}O_2$
	$LiNi_{0.85}Co_{0.15}O_2$	Li_2CO_3		Co_2NiO_4				
Space group	*R*-3*m*	*C*2/*c*		*Fd*-3*m*		*R*-3*m*	*R*-3*m*	*R*-3*m*
Lattice constant								
a (Å)	2.882(27)	8.419(97)		7.983(39)		2.878(00)	2.875(53)	2.874(19)
b (Å)	2.882(27)	4.995(48)		7.983(39)		2.878(00)	2.875(53)	2.874(19)
c (Å)	14.219(86)	6.213(53)		7.983(39)		14.226(14)	14.245(16)	14.267(41)
α	90	90		90		90	90	90
β	90	114.980(83)		90		90	90	90
γ	120	90		90		120	120	120
Cell volume (A3)	102.30(5)	236.90(2)		508.81(8)		102.04(7)	102.00(8)	102.07(2)
Structure parameters								
R_p	8.67					10.9	10.5	11.6
R_{wp}	8.23					10.2	14.5	11.1
Li_{3b}								
x	0	0.179(12)		x		0	0	0
y	0	0.336(57)		x		0	0	0
z	0.5	0.634(94)		x		0.5	0.5	0.5
Occ	0.850(3)	1		x		0.926(3)	0.943(5)	0.935(5)
B	1.872(27)	0.5		x		1.611(40)	2.763(64)	3.175(62)
Ni_{3b}								
x	0	x		x		0	0	0
y	0	x		x		0	0	0
z	0.5	x		x		0.5	0.5	0.5
Occ	0.150(3)	x		x		0.074(3)	0.057(5)	0.065(5)
B	1.872(27)	x		x		1.611(40)	2.763(64)	3.175(62)
Ni_{3a}								
x	0	x		0.5		0	0	0
y	0	x		0.5		0	0	0
z	0	x		0.5		0	0	0
Occ	0.818(4)	x		0.5		0.676(0)	0.593(0)	0.385(0)
B	0.747(61)	x		0.5		0.422(7)	0.406(86)	0.422(88)
Mn_{3a}								
x	x	x		x		0	0	0
y	x	x		x		0	0	0
z	x	x		x		0	0	0
Occ	x	x		x		0.100(0)	0.200(0)	0.400(0)
B	x	x		x		0.422(7)	0.406(86)	0.422(88)
Co_{3a}								
x	0	x		0.125	0.5	0	0	0
y	0	x		0.125	0.5	0	0	0
z	0	x		0.125	0.5	0	0	0
Occ	0.150(0)	x		1	0.5	0.150(0)	0.150(0)	0.150(0)
B	0.747(61)			0.5	0.5	0.422(7)	0.406(86)	0.422(88)
Li_{3a}								
x	0	x		x		0	0	0
y	0	x		x		0	0	0
z	0	x		x		0	0	0
Occ	0.032(0)	x		x		0.074(0)	0.057(0)	0.065(5)
B	0.747(61)	x		x		0.422(7)	0.406(86)	0.422(88)
O								
x	0	0.147(70)	0	0.206(17)		0	0	0
y	0	−0.129(17)	0.296(09)	0.206(17)		0	0	0
z	0.25862(17)	0.334(62)	0.25	0.206(17)		0.25811(17)	0.25851(20)	0.25739(20)
Occ	2.000(0)	1	1	1		2.000(0)	2.000(0)	2.000(0)
B	0.500(0)	0.5	0.5	0.5		1.212(79)	0.459(91)	0.500(0)
C								
x	x	0		x		x	x	x
y	x	0.296(09)		x		x	x	x
z	x	0.25		x		x	x	x
Occ	x	1		x		x	x	x
B	x	0.5		x		x	x	x

The site of Li in Li_2CO_3 is not defined as Li_{3a} and Li_{3b}. Also, the site of Ni in Co_2NiO_4 is not defined as Ni_{3a} and Ni_{3b}.

according to the refinement of the XRD data. Fig. 3 shows the variation in the proportion of Ni^{2+} ions in the lithium layer as the Mn content increases. As the content of Mn increases from 0.1 to 0.4 and the Ni content decreases from 0.75 to 0.45, there is almost no change in the occupation of Ni^{2+} ions in the lithium layer. This differs from a previous finding that the degree of nickel and lithium interlayer mixing increases as the nickel content is reduced [13].

The ratio of I_{003}/I_{104} shows complex variation as the Mn content increases, as shown in Fig. 3. This finding is not consistent with a previously reported research result [14]. Intensity ratios of I_{003}/I_{104} are used as an indication of cation mixing, which expresses a fraction of Ni and Li ion interchange sites in the crystal lattice. A larger I_{003}/I_{104} value implies that the sample is more highly ordered [15]. Fig. 3 shows that a relationship exists between the Ni and Li ion interchange sites and the intensity ratios of I_{003}/I_{104} with the content of Mn in the sample. Lattice parameter *a* decreases, while lattice parameters *c* and *c*/*a* increase as the Mn content increases. The lattice parameter *c* obtained in our study

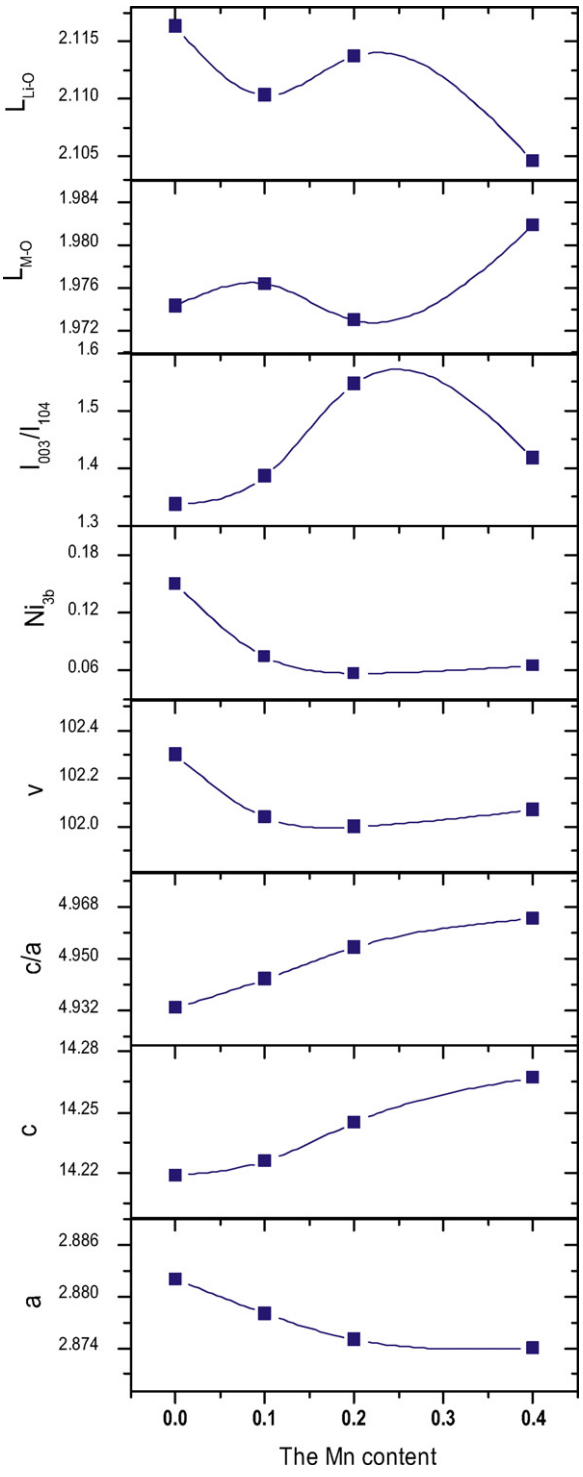

Fig. 3. The variation of Ni^{2+} in the Li layer, the bond lengths of Li–O, M–O, I_{003}/I_{104}, lattice parameters of *a*, *c*, the ratio of *c*/*a* and volume of $LiNi_{0.85-x}Co_{0.15}Mn_xO_2$ as the Mn content increases.

is consistent with that from previously reported work, but lattice parameter *a* is different [16]. The ratio of *c*/*a* increases as the content of Mn in the sample increases, which is consistent with the results of another experiment [15].

Figs. 4–6 show the XPS results for Co $2p_{3/2}$, Ni $2p_{3/2}$ and Mn $2p_{3/2}$ in the materials; their binding energies are summarized in Table 2. The binding energies were obtained by fitting of experimental curves to calculated profiles. The calculated curve profiles were defined as a combination of Gaussian and Lorentzian distributions with an anisotropic contribution, taking into account the asymmetrical shape usually observed for transition metal 2p lines. The Co $2p_{3/2}$ peak from $LiNi_{0.85-x}Co_{0.15}Mn_xO_2$ ($x = 0.1$, 0.2 and 0.4) appeared at 780 eV. This value is close to those of Co^{3+} in $LiNi_{1/3}Mn_{1/3}Co_{1/3}O_2$ and $Li_{1+x}(Ni_zMn_zCo_{1-2z})O_2$ [17,18]. This indicates that the oxidation state of Co in the $LiNi_{0.85-x}Co_{0.15}Mn_xO_2$ samples is +3. For the Ni $2p_{3/2}$ spectra of the $LiNi_{0.85-x}Co_{0.15}Mn_xO_2$ samples, two contributions, one at ca. 853.5 eV for the Ni^{2+} ion and another at ca. 855 eV for the Ni^{3+} ion, were observed. The ratios of Ni^{2+}:(Ni^{2+} + Ni^{3+}) calculated from the results of the XPS study increased considerably as the Mn content increased. It has been reported previously that the ratios of Ni^{2+}:Ni^{3+} increased as the Mn content was increased [16]. The Mn $2p_{3/2}$ spectrum possessed one peak at ca. 642 eV corresponding to the binding energy of Mn^{4+}.

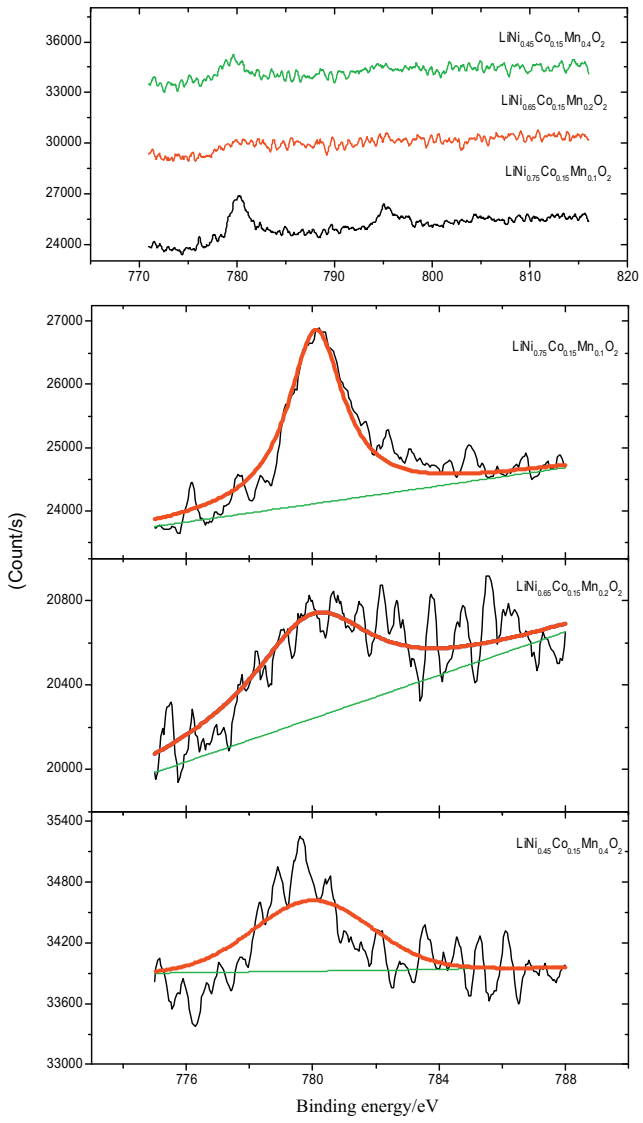

Fig. 4. XPS spectrum of Co $2p_{3/2}$ for the synthesized materials.

Table 2
Binding energies of Co, Ni and Mn for $LiNi_{0.85-x}Co_{0.15}Mn_xO_2$ ($x = 0.1$, 0.2, and 0.4) calculated from the XPS data.

Mn	Co^{3+} (eV)	Ni^{2+} (eV)	Ni^{3+} (eV)	Mn^{4+} (eV)	$Ni^{2+}/(Ni^{2+}+Ni^{3+})$
0.1	780.1	853.5	855.1	642.2	0.10
0.2	780.0	853.5	855.1	642.2	0.24
0.4	780.0	853.5	854.9	642.1	0.69

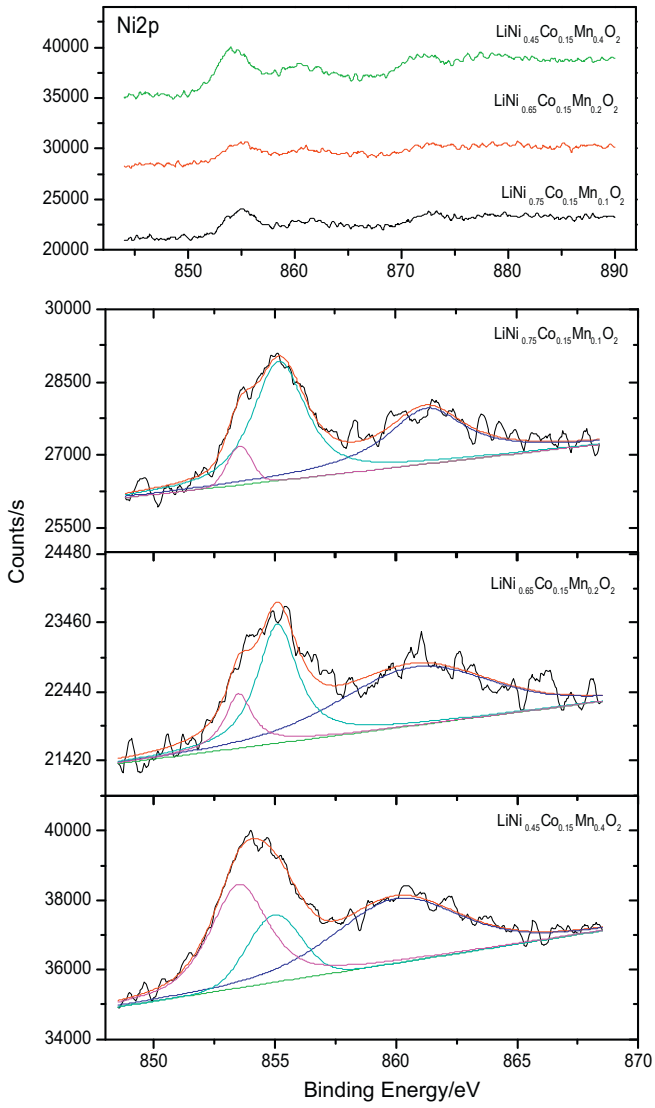

Fig. 5. XPS spectrum of Ni $2p_{3/2}$ for the synthesized materials.

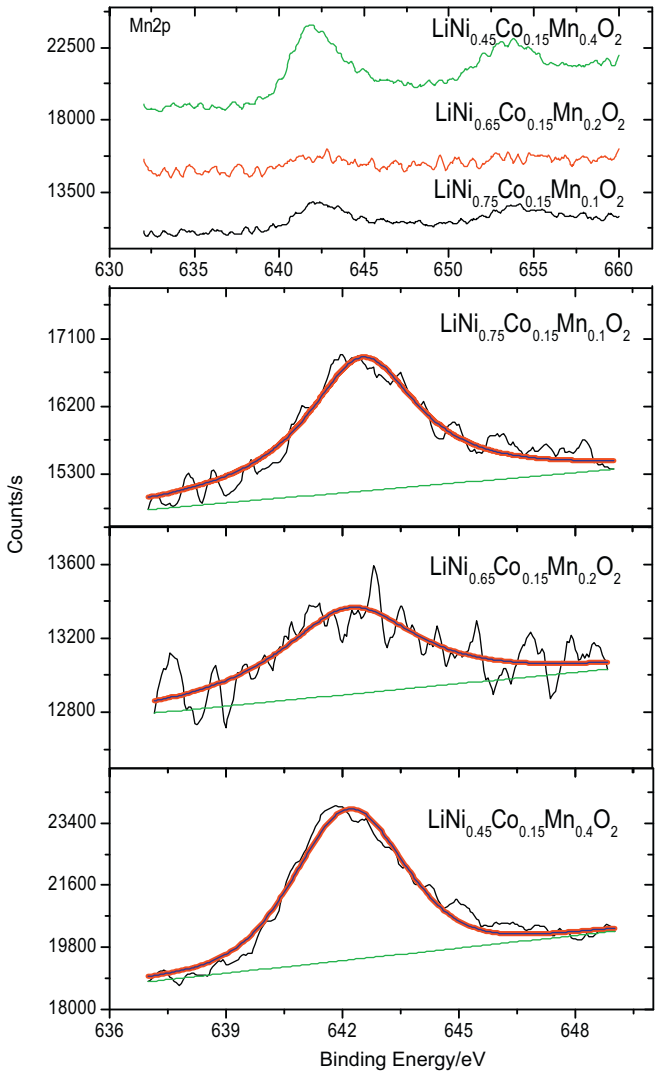

Fig. 6. XPS spectrum of Mn $2p_{3/2}$ for the synthesized materials.

4. Discussion

The oxidation state of Co in $LiMn_xNi_yCo_zO_2$ is typically +3. The Co $2p_{3/2}$ spectra of $Li_{1+x}(Mn_{0.425}Ni_{0.425}Co_{0.15})_{1-x}O_2$ are consistent with the samples containing Co^{3+} ions [18]. The results of XPS indicated that the oxidation state of Co in the $LiNi_{0.85-x}Co_{0.15}Mn_xO_2$ compounds ($x = 0$, 0.1, 0.2 and 0.4) is also +3.

There are two possibilities for the oxidation states of Ni in $LiMn_xNi_yCo_zO_2$ compounds. In layered $LiNi_{0.5}Mn_{0.5}O_2$, charge compensation during charge and discharge is achieved mainly by the oxidation/reduction of Ni^{2+} and Ni^{4+} ions from in situ Ni at the K-edge [19]. Recently X-ray absorption near-edge spectroscopy experiments verified the presence of Ni^{2+} in several compounds of the series $LiNi_xMn_xCo_{1-2x}O_2$ ($0.01 < x < 1/3$) [12]. But, according to the Ni $2p_{3/2}$ XPS, two contributions, one for Ni^{2+} and another for Ni^{3+}, were observed and the ratios of $Ni^{3+}/(Ni^{2+} + Ni^{3+})$ from XPS fitting results were considerably increased with overlithiation [18]. The contribution of the peak corresponding to Ni^{3+} in the Ni $2p_{3/2}$ spectrum is around 93% of the total Ni content for $LiNi_{0.65}Co_{0.25}Mn_{0.1}O_2$. This peak decreases to 61% of the total Ni content for $LiNi_{0.5}Co_{0.25}Mn_{0.25}O_2$, so the ratio of Ni^{2+}/Ni^{3+} increases as the content of Mn in the samples increases [16]. Our experimental results from XPS supported the idea that the Ni ions exist in a mixture of +2 and +3 oxidation states in the $LiNi_{0.85-x}Co_{0.15}Mn_xO_2$ compounds ($x = 0$, 0.1, 0.2 and 0.4). In general, research has shown that the oxidation state of Mn in $LiMn_xNi_yCo_zO_2$ compounds is mostly +4. First-principle calculations have shown that strong interactions between Ni^{2+} and Mn^{4+} ions are favorable. This is supported by the fact that an increased number of Mn^{4+} ions is accompanied by an increased number of Ni^{2+} ions in $LiMn_xNi_yCo_zO_2$ compounds [20]. Therefore, as the content of Mn increases, the ratio of Ni^{2+}:($Ni^{2+} + Ni^{3+}$) increases, which is consistent with the result of XPS data for the $LiNi_{0.85-x}Co_{0.15}Mn_xO_2$ compounds.

As the Mn content increases, the lattice parameters a and c are affected differently according to different researches. Changing the Mn concentration is not a simple substitution reaction. As the Mn content increases, the smaller Ni^{3+} ions transform into the larger Ni^{2+} ions. The percentage of Ni^{2+} increases to balance the smaller radius of the Mn dopant. As a result, the lattice parameter c and the unit cell volume increase as the Mn content increases [15]. The decrease in the value of lattice parameter a is attributed to the increasing Mn^{4+} ion content because Mn^{4+} has a smaller ionic radius in octahedral coordination (0.54 Å) compared with high-spin Mn^{3+} (0.65 Å), low-spin Ni^{3+} (0.56 Å), Ni^{2+} (0.70 Å), high-spin Co^{3+} (0.61 Å) and low-spin Co^{2+} (0.65 Å), all of which might be present in varying levels in these highly complex integrated struc-

Table 3
Calculated bond lengths for $LiNi_{0.85-x}Co_{0.15}Mn_xO_2$ compounds (x = 0, 0.1, 0.2 and 0.4).

	$LiNi_{0.85}Co_{0.15}O_2$	$LiNi_{0.75}Mn_{0.1}Co_{0.15}O_2$	$LiNi_{0.65}Mn_{0.2}Co_{0.15}O_2$	$LiNi_{0.45}Mn_{0.4}Co_{0.15}O_2$
Li_{3b}–O	2.1163(16)	2.1103(16)	2.1137(18)	2.1046(18)
Ni_{3a}–O	1.9743(14)	1.9764(14)	1.9730(15)	1.9818(16)
Ni_{3b}–O	2.1163(16)	2.1103(16)	2.1137(18)	2.1046(18)
Co_{3a}–O	1.9743(14)	1.9764(14)	1.9730(15)	1.9818(16)
Mn_{3a}–O	x	1.9764(14)	1.9730(15)	1.9818(16)
O_1–O_2	2.882(27)	2.8779(99)	2.8755(25)	2.8741(85)

tures [21,22]. The variation of the lattice parameters a and c with changes in the Mn-doping is shown in Fig. 3. Because of the complex substitution effect caused by Mn-doping, the change of the lattice parameters a and c does not directly correlate to the radius change of the ions in $LiNi_{0.85-x}Co_{0.15}Mn_xO_2$. As shown in Fig. 7, transitional elements oxygen octahedron and Li oxygen octahedron share one edge O_1O_2. The variation of L_{M-O} (the length of the metal–oxygen bond) reflects the substitution effect of the changing Mn content. Fig. 3 and Table 3 show the variation of the L_{M-O} and L_{Li-O} as the Mn content increases. When the Mn content is 0.2, L_{M-O} is the smallest. Although the radius of Li and O ions is believed invariable with the changing Mn content, the L_{Li-O} changes as the Mn content varies; L_{M-O} is largest for the compound $LiMn_{0.4}Ni_{0.45}Co_{0.15}O_2$. There is an almost opposing variation extent between L_{M-O} and L_{Li-O} with increasing Mn content according to Fig. 3.

The ^{6}Li MAS NMR spectrum of $^6Li[Ni_{0.02}Mn_{0.02}Co_{0.96}]O_2$ is consistent with the formation of Ni^{2+} and Mn^{4+} clusters within the transition metal layers, even at such low doping levels [12]. When the content of Mn increases from 0 to 0.1, the Ni^{2+} in the Li layer decreases from 15% to 7%; In the short-range, Li ions in the transition metal layer are preferentially surround by Mn ions as revealed by NMR studies [10]. In-plane ordering of lithium and transition metal ions in $Li[Li_{1/9}Ni_{1/3}Mn_{5/9}]O_2$ and Li_2MnO_3 has been evidenced by X-ray diffraction, solid-state nuclear magnetic resonance and extended X-ray absorption fine structure studies [23–25]. When the Mn content increases from 0.1 to 0.4 in the $LiNi_{0.85-x}Co_{0.15}Mn_xO_2$ compounds, the proportion of Ni^{2+} in the Li layer is almost invariable due to the ordering of Li^+ and Mn^{4+}. Although the presence of Ni in the Li layer is believed generally to have detrimental effects in the reversibility of lithium intercalation and the de-intercalation process by impeding Li diffusion in the Li slab space, $Li/LiNi_{0.5}Mn_{0.5}O_2$ cells have shown excellent reversible capacities [26]. This is in contrast to the reversibility found for $Li/Li_{1-z}Ni_{1+z}O_2$ cells, which is very sensitive to extra Ni (z value) in the Li layer [27].

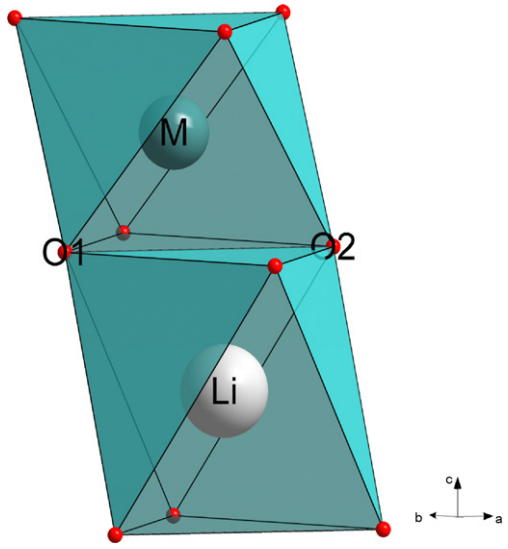

Fig. 7. The transitional elements oxygen octahedron and Li oxygen octahedron.

5. Conclusion

A series of $LiNi_{0.85-x}Mn_xCo_{0.15}O_2$ compounds with x = 0, 0.1, 0.2 and 0.4 were synthesized and characterized. XRD was used for structure examination and XPS was used to determine the formal oxidation states of Ni, Mn and Co in the compounds. The lattice parameter a decreases and the lattice parameter c increases as the Mn content increases. It is suggested that L_{M-O} is representative of the transition metal element radius change as the Mn content increases. The change of L_{M-O} is irregular as Mn increases from 0 to 0.4 due to the different elements, oxidation states and valences about Ni, Co and Mn as the Mn content changes. Although it is believed that L_{Li-O} is invariable with changing Mn content, the experiment shows that a relationship exists between the variation in L_{Li-O} and L_{M-O}. When the content of Mn is 0.1 so the formula is $LiNi_{0.75}Mn_{0.1}Co_{0.15}O_2$, the impure phase found in $LiNi_{0.85}Co_{0.15}O_2$ disappeared. The degree of nickel and lithium interlayer mixing decreases from 15% to 7% as the content of Mn increases from 0 to 0.1. Ni occupation of Li sites is almost invariable as the content of Mn increases from 0.1 to 0.4. The analyses show that the degree of Ni occupation in the Li sites is controlled by the ordering of Mn^{4+} with Ni^{2+} and Mn^{4+} with Li^+.

Acknowledgments

This work was financially supported by Shandong Provincial Natural Science Foundation (grant no. ZR2010EM036) and 863 Program (grant no.2009AA11A106). The authors are grateful to John Lisk for his kind endorsement of the study.

References

[1] J. Morales, C.P. Vicente, J.L. Tirado, Mater. Res. Bull. 25 (1990) 623.
[2] C. Delmas, M. Ménétrier, L. Croguennec, et al., Electrochim. Acta 45 (1999) 243.
[3] C. Delmas, I. Saadoune, Solid State Ionics 370 (1992) 53.
[4] C. Delmas, I. Saadoune, A. Rougier, J. Power Sources 44 (1993) 595.
[5] E. Zhecheva, R. Stoyanova, Solid State Ionics 66 (1993) 143.
[6] A. Ueda, T. Ohzuku, J. Electrochem. Soc. 141 (1994) 2010.
[7] H. Arai, S. Okada, Y. Sakurai, J. Yamaki, Electrochem. Soc. 144 (1997) 3117.
[8] T. Ohzuku, Y. Makimura, Chem. Lett. 30 (2001) 642.
[9] J. Breger, Y.S. Meng, Y. Hinuma, S. Kumar, K. Kang, Y. Shao-Horn, G. Ceder, C.P. Grey, Chem. Mater. 18 (2006) 4768.
[10] C. Pouillerie, E. Suard, C. Delmas, J. Solid State Chem. 158 (2001) 187.
[11] A. Rougier, I. Saadoune, P. Gravereau, F. Willmannb, C. Delmas, Solid State Ionics 90 (1996) 83.
[12] D. Zeng, J. Cabana, J. Bréger, W.S. Yoon, C.P. Grey, Chem. Mater. 19 (2007) 6277.
[13] H. Kbayashi, H. Sakaebe, H. Kageyama, K. Tatsumi, Y. Archi, T. Kamiyama, J. Mater. Chem. 13 (2003) 590.
[14] Z. Liu, A. Yu, J.Y. Lee, J. Power Sources 81 (1999) 416.
[15] S. Jouanneau, K.W. Eberman, L.J. Krause, et al., J. Electrochem. Soc. 150 (2003) A1637.
[16] P.Y. Liao, J.G. Duh, S.R. Sheen, J. Electrochem. Soc. 152 (2005) A1695.
[17] K.M. Shaju, G.V. Sbba Rao, B.V.R. Chowdari, Electrochem. Acta 48 (2002) 145.
[18] J.-M. Kim, N. Kumagi, T.-H. Cho, J. Electrochem. Soc. 155 (2008) A82.
[19] W.S. Yoon, C.P. Grey, M. Balasubramanian, X.Q. Yang, J. McBreen, J. Chem. Mater. 15 (2003) 3161.
[20] Y.S. Meng, G. Ceder, C.P. Grey, W.S. Yoon, Y. Shao-Horn, Electrochem. Solid State Lett. 7 (2004) A155.

[21] M.M. Thackeray, S.-H. Kang, C.S. Johnson, J.T. Vaughey, S.A. Hackney, Electrochem. Commun. 8 (2006) 1531.
[22] C.S. Johnson, N. Li, C. Lefief, J.T. Vaughey, M.M. Thackeray, Chem. Mater. 20 (2008) 6095.
[23] W.S. Yoon, S. Iannopollo, C.P. Grey, D. Carlier, J. Gorman, J. Reed, G. Ceder, Electrochem. Solid State Lett. 7 (2004) A167.
[24] Z.H. Lu, Z.H. Chen, J.R. Dahn, Chem. Mater. 15 (2003) 3214.
[25] W.S. Yoon, N. Kim, X.Q. Yang, J. McBreen, C.P. Grey, J. Power Sources 119–121 (2003) 649.
[26] Y. Makimura, T. Ohzuku, J. Power Sources 119 (2003) 156.
[27] H.H. Li, N. Yabuuchi, Y.S. Meng, S. Kumar, J. Breger, C.P. Grey, Y. Shao-Horn, Chem. Mater. 19 (2007) 2551.